Eur. Phys. J. A **34**, 237–241 (2007)
DOI 10.1140/epja/i2007-10505-4

THE EUROPEAN PHYSICAL JOURNAL A

Letter

Letter

Kaonic hydrogen versus the K^-p low-energy data

A. Cieplý[1,a] and J. Smejkal[2]

[1] Nuclear Physics Institute, 250 68 Řež, Czech Republic
[2] Institute of Experimental and Applied Physics, Czech Technical University, Horská 3a/22, 128 00 Praha 2, Czech Republic

Received: 30 November 2007
Published online: 11 December 2007 –
Communicated by U.-G. Meißner

Abstract. We present an exact solution to the K^--proton bound-state problem formulated in the momentum space. The $1s$ level characteristics of the kaonic hydrogen are computed simultaneously with the available low-energy K^-p data. In the strong-interaction sector the meson-baryon interactions are described by means of an effective (chirally motivated) separable potential and its parameters are fitted to the experimental data.

PACS. 11.80.Gw Multichannel scattering – 12.39.Fe Chiral Lagrangians – 13.75.Jz Kaon-baryon interactions – 36.10.Gv Mesonic atoms and molecules, hyperonic atoms and molecules

1 Introduction

We developed a precise method of computing the meson-nuclear bound states in momentum space. The method was already applied to pionic atoms and its multichannel version was used to calculate the $1s$ level characteristics of pionic hydrogen [1]. In the present work we aim at simultaneous description of both the $1s$ level kaonic bound state and the available experimental data for the K^-p initiated processes.

Until recently the old Deser-Trueman formula [2] was used to determine the strong-interaction energy shift and width (of the $1s$ level) in kaonic hydrogen from the K^-p scattering length and vice versa. Recently, the Deser-Trueman relation was modified to include the isospin effects and electromagnetic corrections [3]. Our exact solution of the K^-p bound-state problem allows to check the precision and limitations of those approximate approaches. However, one should not forget that the strong-interaction part of the scattering length is not a directly measured quantity and its determination from the scattering data is always model dependent.

The treatment of the kaon-nucleon interaction at low energies requires a special care. Unlike the pion-nucleon interaction the $\bar{K}N$ dynamics is strongly influenced by the existence of the $\Lambda(1405)$-resonance, just below the K^-p threshold. This means that the standard chiral perturbation theory is not applicable in this region. Fortunately, one can use non-perturbative coupled-channel techniques to deal with the problem and generate the $\Lambda(1405)$-resonance dynamically. Such approach has proven quite useful and several authors have already applied it to various low-energy meson-baryon processes [4–8]. Whether the recent experimental results on kaonic hydrogen from the DEAR Collaboration [9] are consistent with the older KEK results [10] and whether they fit into the picture drawn by the chiral models represents a question which is addressed by the theory [8,11] as well as by the coming SIDDHARTA experiment.

2 Formalism

Our approach to solving the meson-nuclear bound-state problem in the presence of multiple coupled channels was given in ref. [1]. Here we just remark that the method is based on the construction of the Jost matrix and involves the solution of the Lippman-Schwinger equation for the transition amplitudes between various channels. Bound states in a specific channel then correspond to zeros of the determinant of the Jost matrix at (or close to) the positive part of the imaginary axis in the complex momentum plane. The zeros are computed iteratively and if only the point-like Coulomb potential is considered in the K^-p channel the method reproduces the well-known Bohr energy of the $1s$ level with a precision better than 0.1 eV.

We follow the approach of ref. [4] when constructing the strong-interaction part of the potential matrix. In this

[a] e-mail: cieply@ujf.cas.cz

model the $\Lambda(1405)$-resonance is generated dynamically by solving coupled Lippman-Schwinger equations with input effective (chirally motivated) potentials. The reader should note that our approach differs from the recently more popular on-shell scheme based on the Bethe-Salpeter equation, unitarity relation for the inverse of the T-matrix and on the dimensional regularization of the scalar loop integral [12]. Further, while the authors of ref. [4] restricted themselves only to the first six meson-baryon channels that are open at the $\bar{K}N$ threshold we employ all ten coupled meson-baryon channels: K^-p, $\bar{K}^0n$, $\pi^0\Lambda$, $\pi^+\Sigma^-$, $\pi^0\Sigma^0$, $\pi^-\Sigma^+$, $\eta\Lambda$, $\eta\Sigma^0$, $K^+\Xi^-$, and $K^0\Xi^0$.

The strong-interaction potentials are constructed in such a way that in the Born approximation they give the same (up to $\mathcal{O}(q^2)$) s-wave scattering lengths as are those derived from the underlying chiral Lagrangian. Here we use them in the separable form

$$V_{ij}(k,k') = \sqrt{\frac{1}{2E_i}\frac{M_i}{\omega_i}}\, g_i(k)\, \frac{C_{ij}}{f^2}\, g_j(k') \sqrt{\frac{1}{2E_j}\frac{M_j}{\omega_j}}\ ,$$
$$g_j(k) = \frac{1}{1+(k/\alpha_j)^2}\ , \qquad (1)$$

in which the momenta k and k' refer to the meson-baryon c.m. system in the i and j channels, respectively, and the kinematical factors $\sqrt{M_j/(2E_j\omega_j)}$ guarantee a proper relativistic flux normalization with E_j, M_j and ω_j denoting the meson energy and the baryon mass and energy in the c.m. system of channel j. The off-shell form factors $g_j(k)$ introduce the inverse range radii α_j that characterize the radius of interactions in various channels. Finally, the parameter f stands for the pseudoscalar meson decay constant in the chiral limit and the coupling matrix C_{ij} is determined by chiral $SU(3)$ symmetry and includes terms up to the second order in the meson c.m. kinetic energies. For the first six channels the couplings C_{ij} were listed in [4] and we intend to publish the remaining coefficients in a more elaborate paper [13]. For illustration, we show just the coupling of the elastic K^-p process,

$$C_{K^-p,K^-p} = -E_K - \frac{E_K^2-m_K^2}{2M_0} + \left(F^2+\frac{D^2}{3}\right)\frac{E_K^2}{2M_0}$$
$$+4m_K^2(b_D+b_0) - E_K^2(2d_D+2d_0+d_1). \quad (2)$$

Here m_K and E_K denote the kaon mass and energy in the center-of-mass frame, M_0 stands for the baryon mass in the chiral limit, and the parameters F, D, and b's and d's represent coupling constants that appear in the underlying chiral Lagrangian (see [4] for more details). The origin and relevance of the various terms present in eq. (2) was discussed thoroughly in ref. [7]. In general, the coefficients C_{ij} include contributions from the meson-baryon contact interactions as well as the direct and crossed Born terms. However, in contrast to [7] our model is based on the static (heavy) nucleon approximation adopted by the authors of ref. [4] in which the underlying Lagrangian is expressed in a fixed reference frame.

The potential of eq. (1) is used not only when solving the bound-state problem but we also implement it in the standard Lippman-Schwinger equation and compute the low-energy $\bar{K}N$ cross-sections and branching ratios from the resulting transition amplitudes.

Table 1. The fitted $\bar{K}N$ threshold data.

$\sigma_{\pi N}$ [MeV]	χ^2/N	ΔE_N [eV]	Γ [eV]	γ	R_c	R_n
20	1.33	232	725	2.366	0.657	0.191
30	1.36	262	697	2.365	0.657	0.190
40	1.37	253	710	2.370	0.657	0.189
50	1.40	266	708	2.370	0.658	0.190
exp	–	193(43)	249(150)	2.36(4)	0.664(11)	0.189(15)

3 $\bar{K}N$ data fits

The parameters of the chiral Lagrangian which enter the coefficients C_{ij} and the inverse range radii α_j determining the off-shell behavior of the potentials are to be fitted to the experimental data. Before performing the fits we reduce the number of the fitted parameters in the following way. First, the axial couplings D and F were already fixed in the analysis of semileptonic hyperon decays [14], $D = 0.80$, $F = 0.46$ ($g_A = F + D = 1.26$). Then, we fix the couplings b_D and b_F to satisfy the approximate Gell-Mann formulas for the baryon mass splittings,

$$M_\Xi - M_N = -8b_F(m_K^2-m_\pi^2)\ ,$$
$$M_\Sigma - M_\Lambda = \frac{16}{3}b_D(m_K^2-m_\pi^2)\ , \qquad (3)$$

which gives $b_D = 0.064$ GeV^{-1} and $b_F = -0.209$ GeV^{-1}. Similarly, we determine the coupling b_0 and the baryon chiral mass M_0 from the relations for the pion-nucleon sigma term $\sigma_{\pi N}$ and the proton mass,

$$\sigma_{\pi N} = -2m_\pi^2(2b_0+b_D+b_F),$$
$$M_p = M_0 - 4m_K^2(b_0+b_D-b_F) - 2m_\pi^2(b_0+2b_F). \quad (4)$$

Since the value of the pion-nucleon σ-term is not well determined we enforce four different options, $\sigma_{\pi N} =$ 20–50 MeV, which cover the interval of the values considered by various authors. Finally, we reduce the number of the inverse ranges α_j to only five: α_{KN}, $\alpha_{\pi\Lambda}$, $\alpha_{\pi\Sigma}$, $\alpha_{\eta\Lambda/\Sigma}$ (for both the $\eta\Lambda$ and $\eta\Sigma$ channels) and $\alpha_{K\Xi}$. This leaves us with 11 free parameters: the five inverse ranges, the meson-baryon chiral coupling f, and five more low-energy constants from the second-order chiral Lagrangian denoted by d_D, d_F, d_0, d_1, and d_2.

The fitted low-energy $\bar{K}N$ data include the three precisely measured threshold branching ratios [15]

$$\gamma = \frac{\sigma(K^-p\to\pi^+\Sigma^-)}{\sigma(K^-p\to\pi^-\Sigma^+)} = 2.36\pm0.04,$$
$$R_c = \frac{\sigma(K^-p\to\text{charged particles})}{\sigma(K^-p\to\text{all})} = 0.664\pm0.011,$$
$$R_n = \frac{\sigma(K^-p\to\pi^0\Lambda)}{\sigma(K^-p\to\text{all neutral states})} = 0.189\pm0.015, \quad (5)$$

Table 2. Chiral Lagrangian parameters (b_0 and d's in 1/GeV).

$\sigma_{\pi N}$ [MeV]	b_0	M_0 [MeV]	$a^+_{\pi N}$ [m_π^{-1}]	f [MeV]	d_0	d_D	d_F	d_1	d_2
20	−0.190	997	−0.016	108.6	−0.385	−0.368	−0.817	0.396	0.152
30	−0.321	864	0.001	100.0	−0.354	−0.206	−0.522	0.406	−0.211
40	−0.453	729	0.006	108.9	−0.484	−0.151	−0.459	0.448	−0.280
50	−0.584	594	0.007	108.8	−0.747	−0.092	−0.429	0.567	−0.349
27 [4]	−0.279	910	−0.002	94.5	−0.40	−0.24	−0.43	0.28	−0.62

Table 3. Inverse range parameters α_j (in MeV).

$\sigma_{\pi N}$ [MeV]	α_{KN}	$\alpha_{\pi\Lambda}$	$\alpha_{\pi\Sigma}$	$\alpha_{\eta\Lambda/\Sigma}$	$\alpha_{K\Xi}$
20	610	209	570	1100	530
30	647	262	535	308	21
40	653	320	618	281	89
50	594	370	610	342	124
27 [4]	760	300	450	–	–

and K^-p-initiated total cross-sections. For the later ones we consider only the experimental data taken at the kaon laboratory momenta $p_{LAB} = 110$ MeV (for the K^-p, $\bar{K}^0n$, $\pi^+\Sigma^-$, $\pi^-\Sigma^+$ final states) and at $p_{LAB} = 200$ MeV (for the same four channels plus $\pi^0\Lambda$ and $\pi^0\Sigma^0$). Our results show that the inclusion of the cross-section data taken at other kaon momenta is not necessary since the fit at just 1–2 points fixes the cross-section magnitude and the energy dependence is reproduced nicely by the model. Finally, we include the DEAR results [9] on the strong-interaction shift ΔE_N and the width Γ of the $1s$ level in kaonic hydrogen:

$$\Delta E_N(1s) = (193 \pm 43)\ \text{eV}, \quad \Gamma(1s) = (249 \pm 150)\ \text{eV}. \quad (6)$$

Thus, we end up with a total of 15 data points in our fits.

Our results are summarized in tables 1–3. The first table shows the results of our χ^2 fits compared with the relevant experimental data. The resulting χ^2 per data point indicate satisfactory fits. It is worth noting that their quality and the computed values do not depend much on the exact value of the $\sigma_{\pi N}$ term. Tables 2 and 3 show the fitted parameters of the chiral Lagrangian and the inverse range parameters α_j. The last rows in the tables compare our values with those determined in ref. [4]. We remind the reader that the parameter b_0 and the baryon mass in the chiral limit were not fitted to the data and are given in the second and third column of table 2 only to visualize their respective values corresponding to the selected $\sigma_{\pi N}$ term. The πN isospin-even scattering length $a^+_{\pi N}$ shown in the fourth column of table 2 was not included in our fits either but we feel that its presentation is important and deserves some comments.

The goal of the present work was to check the compatibility of the DEAR kaonic hydrogen data with the low-energy K^-p cross-sections and branching ratios. Therefore, we have not included in our fits the $\Lambda(1405)$ mass spectrum and other processes considered, *e.g.*, in ref. [8]. In fact, the low-energy constants involved in the fits should be also constrained by other observables calculated within the framework of ChPT involving the same meson-baryon Lagrangian. The spectrum of baryon masses and the πN isospin-even scattering length may come to one's mind in this respect. The later quantity to order q^3 is given by [16]:

$$a^+_{\pi N} = \frac{1}{4\pi(1+m_\pi/M_N)} \times \left[\frac{m_\pi^2}{f^2}(-2b_D - 2b_F - 4b_0 + d_D + d_F + 2d_0) - \frac{m_\pi^2}{f^2}\frac{g_A^2}{4M_N} + \frac{3g_A^2 m_\pi^3}{64\pi f^4}\right]. \quad (7)$$

Since the experimental value of $a^+_{\pi N}$ is practically consistent with zero, $a^+_{0+} = -(0.25 \pm 0.49)\cdot 10^{-2}\, m_\pi^{-1}$ [17], it is encouraging to note the mostly negative signs of the d-parameters that cancel the positive contributions due to the b terms and the q^3 correction represented by the last term in eq. (7). As a smaller $\sigma_{\pi N}$ term means a smaller absolute value of the negative parameter b_0 (and hence a smaller positive contribution due to the b_0 term in $a^+_{\pi N}$) it is not surprising that the computed πN scattering length is becoming negative for too low $\sigma_{\pi N}$ terms. Anyway, it is interesting that our fits aimed at the $\bar{K}N$ interactions allow for so good reproduction of the πN quantity. Specifically, the parameter set obtained in the fit for $\sigma_{\pi N} = 30$ MeV gives $a^+_{\pi N}$ in a nice agreement with experiment while the χ^2/N is only slightly inferior to our best fit. Many other authors (*e.g.*, [4] or [8]) include the $a^+_{\pi N}$ value directly in their fits. The d couplings (of the second-order chiral Lagrangian) contribute to the contact meson-baryon interactions in the second order of meson momenta. Although our fits confirm their mostly negative signs it is difficult to come to any conclusions concerning their values. The fact that even the sign of d_2 is not well determined in our analysis speaks for itself.

We have also tried to perform fits with the b-parameters taken from the analysis of the baryon mass spectrum [18] and with only the current algebra (Weinberg-Tomozawa) term contributing to the C_{ij} coefficients (the approach adopted in ref. [5]). Unfortunately, we were not able to achieve satisfactory results in those cases. Thus, we conclude that the low-energy constants derived in the analysis of baryon masses are not suitable in the sector of meson-baryon interactions and that the inclusion of the q^2 terms is necessary for a good description of the $\bar{K}N$ data. The later point is in agreement with the analysis of ref. [7].

The inverse range parameters given in table 3 are in line with our expectations. The values corresponding to the open channels $\bar{K}N$, $\pi\Lambda$ and $\pi\Sigma$ seem to be well de-

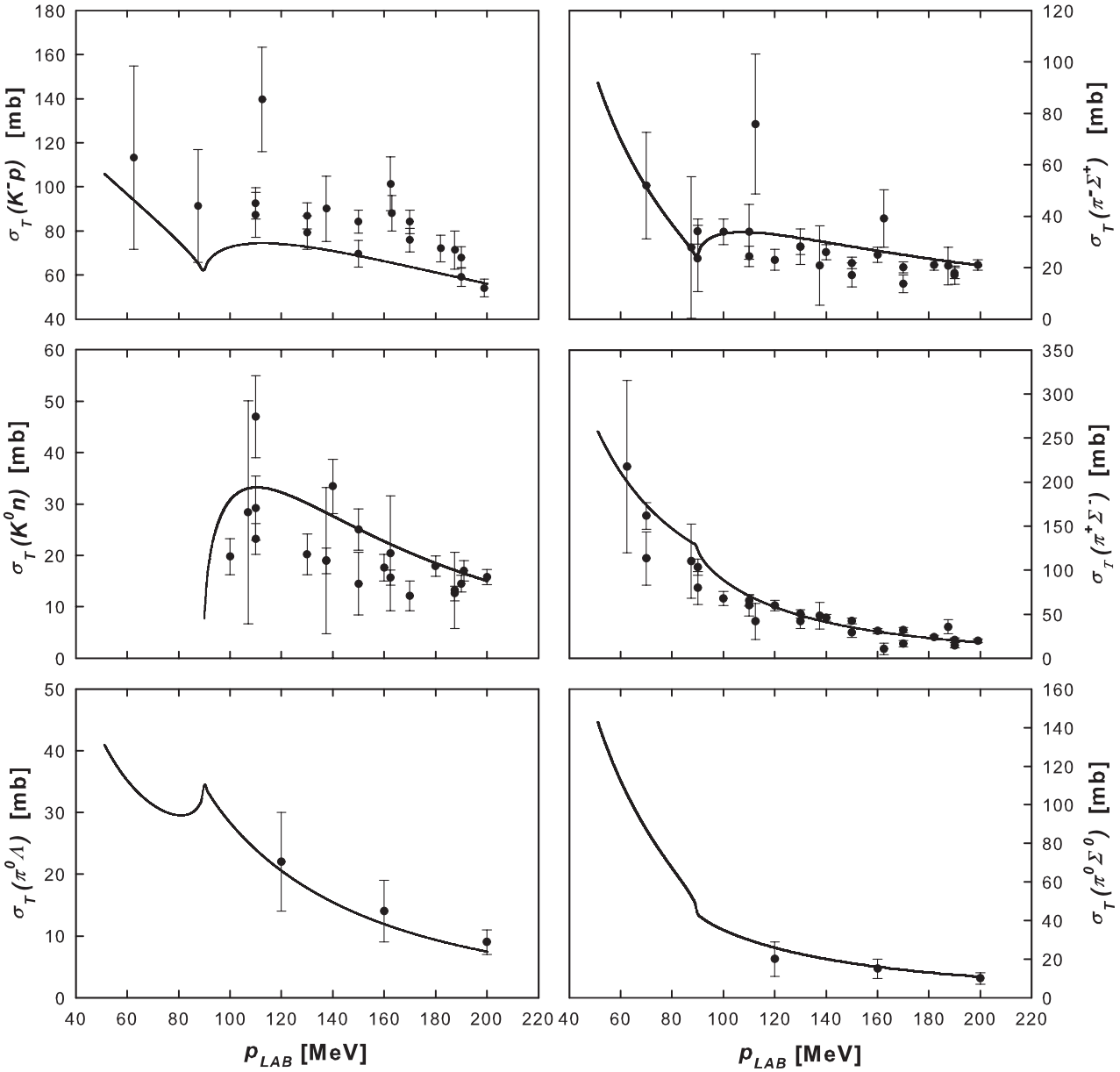

Fig. 1. Total cross-sections for K^-p scattering and reactions to the meson-baryon channels open at low kaon laboratory momenta p_{LAB}. The experimental data are the same as those compiled in fig. 1 of ref. [4].

termined and show only a moderate dependence on the adopted value of the $\sigma_{\pi N}$ term. In general, the ranges obtained for the open channels correspond to the t-channel exchanges that are believed to dominate the interactions. On the other hand, the range of interactions in the closed channels is not well defined in the fits and the fitted values $\alpha_{\eta\Lambda/\Sigma}$ and $\alpha_{K\Xi}$ exhibit relatively large statistical errors. This feature also justifies our use of only one range parameter for both η channels.

In fig. 1 we present the low-energy K^-p initiated cross-sections calculated using our best fit with $\sigma_{\pi N} = 20$ MeV. The results obtained for the other adopted values of $\sigma_{\pi N}$ are quite similar, therefore we decided not to include them in the figure. Though we declined from using all experimental data in our fits and took only the data points available for the selected kaon laboratory momenta $p_{LAB} = 110$ MeV and $p_{LAB} = 200$ MeV, the description of the data is quite good. Specifically, we do not observe the lowering of the calculated cross-sections in the elastic K^-p channel reported by Borasoy *et al.* [7] for their fits including the kaonic hydrogen characteristics. Though our K^-p cross-sections are also slightly below the experimental data the difference is not significant. In addition, the inclusion of electromagnetic corrections discussed in ref. [7] should partly improve the description for the lowest kaon momenta.

Finally, let us turn our attention to the calculated characteristics of the 1s level in kaonic hydrogen. The strong-interaction energy shift of the 1s level in kaonic hydrogen is reproduced well but we were not able to get a satisfac-

Table 4. Precision of the Deser-Trueman formula. The complex energies $\Delta E_N - (\mathrm{i}/2)\Gamma$ are given for the approximate DT and MDT formulas and compared with our computed "exact" values.

a_{K^-p} [fm]		$\Delta E_N - (\mathrm{i}/2)\Gamma$ [eV]
$-0.50 + \mathrm{i}\,1.01$	DT	$207 - (\mathrm{i}/2)\,832$
	MDT	$251 - (\mathrm{i}/2)\,714$
	exact	$232 - (\mathrm{i}/2)\,725$
$-0.60 + \mathrm{i}\,1.01$	DT	$247 - (\mathrm{i}/2)\,830$
	MDT	$285 - (\mathrm{i}/2)\,689$
	exact	$266 - (\mathrm{i}/2)\,708$

tory fit of the 1s level energy width as our results are significantly larger than the experimental value. This result is in line with the conclusions reached by Borasoy, Meissner and Nissler [11] on the basis of their comprehensive analysis of the K^-p scattering length from scattering experiments. However, when considering the interval of three standard deviations and also the older KEK results [10] (which give less precise but larger width) we cannot conclude that kaonic hydrogen measurements contradict the other low-energy $\bar{K}N$ data.

In table 4 we compare our results (for $\sigma_{\pi N} = 20$ and 50 MeV) for the 1s level characteristics in kaonic hydrogen with the approximate values determined from the K^-p scattering lengths a_{K^-p}. The later quantity is obtained from the multiple-channel calculation that uses the same parametrization of the strong-interaction potential, eq. (1). The 1s level complex energies are shown for: the standard Deser-Trueman formula (DT) [2], the modified Deser-Trueman formula (MDT) [3] (see also ref. [7] for the relations used to obtain the DT and MDT values) and our "exact" solution of the bound-state problem. The results obtained for $\sigma_{\pi N} = 30$ and 40 MeV are quite similar (with almost identical K^-p scattering lengths), so we did not include them in the table in order to keep the presentation more transparent. Since the numerical precision of determining the bound-state energy by our method is better than 0.1 eV, the discrepancy between the "MDT" and the "exact" values should be attributed to higher-order corrections not considered in the derivation of MDT. In fact, the correction due to Coulomb interaction is taken only in its leading order in the MDT formula. The inclusion of more terms of the relevant geometric series would bring the MDT value into a better agreement with our exact solution [19].

4 Conclusions

We have computed the characteristics of kaonic hydrogen exactly and compared the results (the 1s level energy shift and width) with the values determined from the K^-p scattering length by means of using the standard Deser-Trueman formula and its modified version which includes the corrections due to electromagnetic effects. It looks that the approximate DT formula gives the 1s energy level strong-interaction shift and width about 10% and 15% off the exactly computed values, respectively. Although the modified DT formula does much better job on account of the width, the energy level shift remains about 10% off the exact value that lies approximately in the middle between the DT and MDT values. In view of the current level of the experimental precision, the use of the modified DT formula is sufficient. Nevertheless, the situation may change after the coming SIDDHARTA experiment being prepared in Frascati.

An effective chirally motivated separable potential was used in simultaneous fits of the low-energy K^-p cross-sections, the threshold branching ratios and the characteristics of kaonic hydrogen. The fits are quite satisfactory except the 1s level energy width being much larger than the experimental value. In view of the fact that the experimental precision of the kaonic hydrogen data is still rather low one cannot say that the data contradict the chirally motivated model used to describe the low-energy meson-baryon interactions. However, as the opposite statement cannot be made either we should wait for the new experiment to clarify the situation.

AC acknowledges the financial support from the GA AVCR grant A100480617. The work of JS was supported by the Research Program *Fundamental experiments in the physics of the microworld* No. 6840770029 of the Ministry of Education, Youth and Sports of the Czech Republic.

References

1. A. Cieplý, R. Mach, Nucl. Phys. A **609**, 377 (1996).
2. S. Deser, M.L. Goldberger, K. Baumann, W. Thirring, Phys. Rev. **96**, 774 (1954); T.L. Trueman, Nucl. Phys. **26**, 57 (1961).
3. U.-G. Meissner, U. Raha, A. Rusetsky, Eur. Phys. J. C **35**, 349 (2004).
4. N. Kaiser, P.B. Siegel, W. Weise, Nucl. Phys. A **594**, 325 (1995).
5. E. Oset, A. Ramos, Nucl. Phys. A **635**, 99 (1998).
6. A. Cieplý, E. Friedman, A. Gal, J. Mares, Nucl. Phys. A **696**, 173 (2001).
7. B. Borasoy, R. Nissler, W. Weise, Eur. Phys. J. A **25**, 79 (2005).
8. J.A. Oller, Eur. Phys. J. A **28**, 63 (2006).
9. DEAR Collaboration (G. Beer *et al.*), Phys. Rev. Lett. **94**, 212302 (2005).
10. M. Iwasaki *et al.*, Phys. Rev. Lett. **78**, 3067 (1997); T.M. Ito *et al.*, Phys. Rev. C **58**, 2366 (1998).
11. B. Borasoy, U.-G. Meissner, R. Nissler, Phys. Rev. C **74**, 055201 (2006).
12. J.A. Oller, U.-G. Meissner, Phys. Lett. B **500**, 263 (2001).
13. A. Cieplý, J. Smejkal, in preparation.
14. P.G. Ratcliffe, Phys. Rev. D **59**, 014038 (1999).
15. A.D. Martin, Nucl. Phys. B **179**, 33 (1981) and earlier references cited therein.
16. V. Bernard, N. Kaiser, U.-G. Meissner, Phys. Lett. B **309**, 421 (1993).
17. H.C. Schröder *et al.*, Phys. Lett. B **469**, 25 (1999).
18. B. Borasoy, U.-G. Meissner, Ann. Phys. **254**, 192 (1997).
19. A. Rusetsky, a private communication during the *MENU 2007 Conference* (2007).